Changes in RR Series Characteristics during Atrial Fibrillation: An AV Node Simulation Study

Felix Plappert[1], Mikael Wallman[2], Pyotr Platonov[3], Frida Sandberg[1]

[1] Department of Biomedical Engineering, Lund University, Lund, Sweden
[2] Fraunhofer-Chalmers Centre, Department of Systems and Data Analysis, Sweden
[3] Department of Cardiology, Clinical Sciences, Lund University, Lund, Sweden

Abstract

The atrioventricular node (AVN) plays an important role in rate control during atrial fibrillation (AF). To further our understanding of the AVN function in AF, we present a model-based study, relating AVN electrophysiological characteristics to changes in RR series characteristics observed during treatment with rate control drugs. The dual-pathway physiology of the AVN was modelled using a network of nodes. The atrial impulse series was modelled with a Pearson Type IV distribution. Simulations were performed with randomly generated model parameters based on clinically observed ranges and the heart rate, variability and irregularity of the resulting RR series were quantified by their mean, rmssd and sample entropy, respectively. Analysis using linear regression showed that an increase in the RR mean was predominantly associated with an increase in the refractory period of the slow pathway, whereas changes in RR variability and RR irregularity were associated with changes in conduction delay. Notably, changes in the mean and standard deviation of the atrial impulse intervals were associated with changes in RR irregularity but not with changes in RR variability. Our results suggest that changes in RR series dynamics observed in response to rate control drugs reflect changes in the atrial electrical activity and AV conduction delay, however the results needs to be verified with clinical data.

1. Introduction

Atrial fibrillation (AF) is the most common supraventricular tachyarrhythmia with an estimated prevalence between 2% and 4% of the global population [1]. Atrial fibrillation is characterized by uncoordinated atrial electrical activation resulting in ineffective atrial contraction. With AF being linked to substantial morbidity and mortality and its prevalence being expected to increase, the management of AF has been an ongoing research endeavor.

The atrioventricular node (AVN) is essential for AF management. During AF, the AVN filters the uncoordinated atrial impulse series that is causing the ineffective atrial contraction and is consequently protecting the ventricles. Utilizing and optimizing the AVN's ability to filter atrial impulses is therefore an integral part in improving AF management. One such approach is the use of rate control drugs [2] with the aim to maintain a heart rate below 110 bpm [1]. In general, we know the electrophysiological effects and the likely therapeutic mechanisms for various classes of rate control drugs [2]. In practice, however, the resulting adaptation of the AV nodal physiology during AF with the causality between atrial and ventricular impulses is not fully understood [3]. Thus, unraveling the complex AV nodal physiology may advance the management of AF.

Characteristic for the AVN is its dual-pathway physiology enabling a parallel excitation propagation of impulses with different electrophysiological properties [4]. For example, the slow pathway (SP) has a longer conduction delay and shorter refractory period compared to the fast pathway (FP) [4]. Furthermore, the refractory period and conduction delay are dynamic and depend on the recent history of conducted and blocked impulses in the AV nodal tissue [4, 5]. Even though the ventricular RR series provides insights into the AVN function, the RR series alone is often insufficient to reconstruct the complex dual-pathway physiology. A few human AVN models have been proposed, ranging from simplified statistical models [6] to detailed biophysical descriptions [7]. Here, we are developing an AVN model, based on [8], to analyze the complex AV nodal physiology through simulation. In this work, we focus on the contribution of individual model parameters to changes in RR series characteristics during AF.

2. Methods

2.1. Model Description

The AVN is modelled by a network of M nodes n_j, with $j = 1, ..., M$ [8]. Each node represents a segment of the

AVN and comprises an individual refractory period and conduction delay. An impulse can either be conducted or blocked by a node, based on the interval Δt_i between the current impulse arrival time t_i and the end of the previous refractory period. The impulse is conducted if this interval Δt_i is positive, otherwise the refractory period is ongoing and the impulse is blocked. If an impulse is conducted, the refractory period R_i and conduction delay D_i of the current node i are updated according to Eq. (1)–(3). The conduction delay describes the time delay until the current impulse arrives at all adjacent nodes.

$$R_i(\Delta t_i) = R_{min} + \Delta R \left(1 - e^{-\Delta t_i/\tau_R}\right) \quad (1)$$

$$D_i(\Delta t_i) = D_{min} + \Delta D e^{-\Delta t_i/\tau_D} \quad (2)$$

$$\Delta t_i = t_i - t_{i-1} - R_{i-1} \quad (3)$$

The model describes the dual-pathway physiology with two chains of 10 nodes each. The last nodes of the FP and SP are connected to allow for the simulation of retrograde conduction. Furthermore, the two last nodes are connected to an additional end node (EN). In total, the model consists of 21 nodes with each node characterized by $[R^P_{min}, \Delta R^P, \tau^P_R, D^P_{min}, \Delta D^P, \tau^P_D]$ with $P \in \{FP, SP, EN\}$.

The AVN model processes the impulse propagation chronologically and node by node, using a priority queue of nodes, sorted by impulse arrival time. Details can be found in [8]. The input to the AVN model is a series of atrial activation (AA) intervals. The priority queue is initialized with the impulses from the AA interval series arriving at the first node of each pathway. As the impulses are conducted to adjacent nodes, new entries are added to the priority queue. The output of the AVN model is a series of impulses activating the ventricles.

2.2. Simulation

The AA interval series during AF is modelled using a Pearson Type IV distribution [9]. The distribution requires four parameters, namely the mean μ, standard deviation σ, skewness γ and kurtosis κ. For each simulation, an atrial impulse series with 30 000 AA intervals was generated, with μ randomly drawn from $\mathcal{U}[100, 250]$ ms, σ randomly drawn from $\mathcal{U}[15, 30]$ ms, and γ and κ set to 1 and 6, respectively. Only AA intervals larger than 0 ms were included in the atrial impulse series.

The model parameters of FP and SP were randomly drawn from uniform distributions while the parameters of EN were set to constant values according to Table 1. The generation of model parameters was repeated 3 500 000 times, each creating a different set of model parameters. Compared to the SP, the FP is assumed to have a higher refractory period $R^{FP}_i(\Delta t_i) > R^{SP}_i(\Delta t_i)$ and lower conduction delay $D^{FP}_i(\Delta t_i) < D^{SP}_i(\Delta t_i)$ for all intervals Δt_i. Due to this criterion, 64% of the parameter sets were excluded.

Table 1. Model parameters used for the simulations.

Parameters	FP (in ms)	SP (in ms)	EN (in ms)
R_{min}	$\mathcal{U}[250, 600]$	$\mathcal{U}[250, 600]$	250
ΔR	$\mathcal{U}[0, 600]$	$\mathcal{U}[0, 600]$	0
τ_R	$\mathcal{U}[50, 300]$	$\mathcal{U}[50, 300]$	1
D_{min}	$\mathcal{U}[0, 30]$	$\mathcal{U}[0, 30]$	0
ΔD	$\mathcal{U}[0, 75]$	$\mathcal{U}[0, 75]$	0
τ_D	$\mathcal{U}[50, 300]$	$\mathcal{U}[50, 300]$	1

One simulation was performed for each of the remaining model parameter sets. After each simulation, an RR interval series RR_j with $j = 1, ..., N$ and $N = 2\,000$ was computed from the time intervals between the first $N + 1$ impulses that leave the AVN model. Using the RR interval series, the mean of the RR intervals ($\overline{RR}$), the root mean square of successive RR interval differences (RR_V, variability) and the sample entropy of the RR series (RR_I, irregularity) were computed according to Eq. (4)–(6) [10].

$$\overline{RR} = \frac{1}{N} \sum_{j=1}^{N} RR_j \quad (4)$$

$$RR_V = \sqrt{\frac{1}{N-1} \sum_{j=1}^{N-1} \left(RR_{j+1} - RR_j\right)^2} \quad (5)$$

$$RR_I = -\ln \left(\frac{\sum_{i=1}^{N-m} \sum_{j=1, j\neq i}^{N-m} b^{m+1}_{i,j}(r)}{\sum_{i=1}^{N-m} \sum_{j=1, j\neq i}^{N-m} b^{m}_{i,j}(r)} \right) \quad (6)$$

For the computation of the sample entropy RR_I, $N - l + 1$ vectors of length l are formed $V^l_i = \{RR_i, RR_{i+1}, ..., RR_{i+l}\}$. The variable $b^l_{i,j}(r)$ with $l \in \{m, m + 1\}$ has the value 1 if the maximum absolute distance between corresponding scalar elements in the vectors V^l_i and V^l_j is below the tolerance r times the standard deviation of the RR interval series, otherwise the value is zero. In this study, the parameters were set to $m = 2$ and $r = 0.2$.

Parameter sets resulting in $\overline{RR}$ larger than 1 000 ms or smaller than 300 ms, corresponding to heart rates below 60 bpm or above 200 bpm, were excluded. Due to this criterion, 13.8% of the simulations were excluded. Consequently, the parameter sets and resulting time series measures of $K = 1\,087\,000$ simulations were used for the linear regression analysis.

2.3. Linear Regression Analysis

A linear regression approach was used to investigate the relative importance of each model parameter for the result-

ing RR series characteristics according to Eq. (7).

$$\hat{\boldsymbol{\beta}} = \left(\boldsymbol{X}^T\boldsymbol{X}\right)^{-1}\boldsymbol{X}^T\boldsymbol{Y} \quad (7)$$

The model parameter sets were normalized, so that each model parameter had a zero-mean and unit variance distribution, and a K-by-14 matrix $\boldsymbol{X}$ of predictors was constructed with the k:th row $\boldsymbol{X}(k) = [\widetilde{R}^{SP}_{min}(k),\ \Delta\widetilde{R}^{SP}(k),\ \widetilde{\tau}^{SP}_{R}(k),\ \widetilde{R}^{FP}_{min}(k),\ \Delta\widetilde{R}^{FP}(k), \widetilde{\tau}^{FP}_{R}(k), \widetilde{D}^{SP}_{min}(k), \Delta\widetilde{D}^{SP}(k), \widetilde{\tau}^{SP}_{D}(k), \widetilde{D}^{FP}_{min}(k), \Delta\widetilde{D}^{FP}(k), \widetilde{\tau}^{FP}_{D}(k), \widetilde{\mu}(k), \widetilde{\sigma}(k)]$ with $k = 1, ..., K$. Similar to the matrix $\boldsymbol{X}$, the time series measures were normalized, so that each measure has a zero-mean and unit variance distribution, and a K-by-3 matrix $\boldsymbol{Y}$ of responses was constructed with the k:th row $\boldsymbol{Y}(k) = [\overline{RR}(k), RR_V(k), RR_I(k)]$ with $k = 1, ..., K$. The resulting 14-by-3 matrix $\hat{\boldsymbol{\beta}}$ of regression coefficients describing the linear relationship between the variance of the input and output parameters.

The R^2 statistic was computed according to Eq. (8), resulting in a 1-by-3 vector $\boldsymbol{R^2}$ with $\hat{\boldsymbol{Y}}(k) = \boldsymbol{X}(k)\hat{\boldsymbol{\beta}}$ and $\overline{\boldsymbol{Y}} = \frac{1}{K}\sum_{k=1}^{K}\boldsymbol{Y}(k)$.

$$\boldsymbol{R^2} = \left(1 - \frac{\sum_{k=1}^{K}\left(\boldsymbol{Y}(k) - \hat{\boldsymbol{Y}}(k)\right)^2}{\sum_{k=1}^{K}\left(\boldsymbol{Y}(k) - \overline{\boldsymbol{Y}}\right)^2}\right) \cdot 100\,\%, \quad (8)$$

The three parameters in $\boldsymbol{R^2}$ quantify how well the linear regression model can predict the data for $\overline{RR}(k)$, $RR_V(k)$ and $RR_I(k)$.

3. Results

The regression coefficients $\hat{\boldsymbol{\beta}}$ are presented in Figure 1. According to the linear regression analysis, changes in the mean of the RR series $\overline{RR}$ were predominantly associated with changes in the refractory period parameters of the SP with the three largest values of $\hat{\boldsymbol{\beta}}$ obtained for ΔR^{SP}, R^{SP}_{min} and τ^{SP}_{R}. In contrast, the changes in the variability of the RR series, represented by RR_V, were associated with a broader set of model parameters. The largest $\hat{\boldsymbol{\beta}}$ was obtained for ΔR^{SP} and the conduction delay parameters of both pathways had a similar contribution but in opposite directions; increasing values of D^{SP}_{min} and ΔD^{SP} were associated to increasing RR_V whereas increasing values of D^{FP}_{min} and ΔD^{FP} were associated to decreasing RR_V. The changes in the irregularity of the RR series, represented by RR_I, were also associated with a broad set of model parameters. The largest contribution came from variation in SP refractoriness and conduction delay ΔR^{SP} and ΔD^{SP} and the AA interval series parameters σ and μ, where shorter and more varying AA intervals were associated to more irregular RR series. The R^2 value for the linear regression model was 89.2% for $\overline{RR}$, 34.6% for RR_V and 41.5% for RR_I.

The percentage of blocked impulses were found to decrease with increasing μ (Figure 2). Conduction mainly occured through the SP, with a median of 11.3% for $\mu =$ 100 ms and 33.4% for $\mu = 250$ ms compared to 1.8% for $\mu = 100$ ms and 8.2% for $\mu = 250$ ms for the FP.

4. Discussion and Conclusion

In previous work on the network model [8], the AA interval series was modelled as a Poisson process. However, based on results of Climent et al. [9], a Pearson Type IV distribution better reproduces the statistical properties of the AA interval series during AF and was therefore chosen in this study. For the regression analysis, the skewness and kurtosis were set to fixed values, as they had little impact on the regression coefficients (data not shown).

The length of the RR interval series was chosen to be 2 000, as this corresponds to a typical clinical time scale of a 15–25 min ECG recording. Moreover, simulation results for RR series with 2 000 intervals demonstrated a reasonable trade-off between accuracy and computation time (data not shown).

When excluding data sets from further analysis, the upper limit of $\overline{RR}$ was chosen to be 1 000 ms, corresponding to a heart rate below 60 bpm. For such low heart rates, the pacemaker function of the AVN which is not incorporated in the present model, would have significant impact [4]. The lower limit was chosen based on a reported minimum refractory period in the bundle branches of around 300 ms [11]. Most parameter sets were excluded due to slow heart rate, whereas 25 out of nearly 175 000 parameter sets were excluded based on their $\overline{RR}$ below 300 ms.

The random sampling of the model parameters allows for a high variation between the parameter sets to achieve a large coverage of possible physiological parameter sets. The individual variation was large and for this reason, the linear regression analysis was performed with a large amount of parameter sets.

The regression coefficients for $\overline{RR}$ indicate that a reduction in the mean heart rate is mainly associated with an increase in the refractory period of the SP. The regression coefficients of RR_V suggest that the conduction delay in both FP and SP are important determinants of RR series variability, whereas the regression coefficients of RR_I suggest that increased and more varying atrial activation rates are associated with increased RR series irregularity. Whereas increased RR variability has been previously reported in response to Ca^{+}-blocker and beta-blocker treatment, only beta-blockers were found to increase RR irregularity [12]. Our results suggest that these changes in RR series characteristics are linked to increased SP refractoriness, and that the differences between beta-blockers and

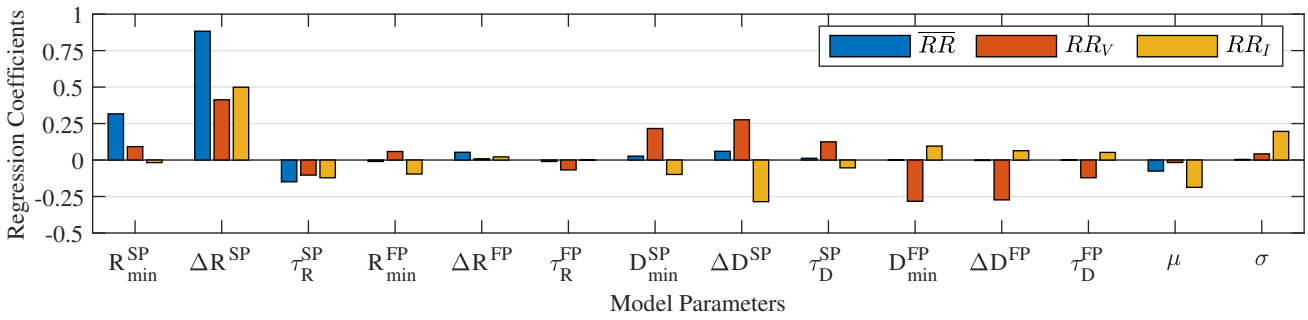

Figure 1. Linear regression coefficients of 14 model parameters for the three RR series measures, namely the mean of the RR intervals ($\overline{RR}$, blue), the root mean square of successive RR interval differences (RR_V, variability, red) and the sample entropy of the RR series (RR_I, irregularity, yellow).

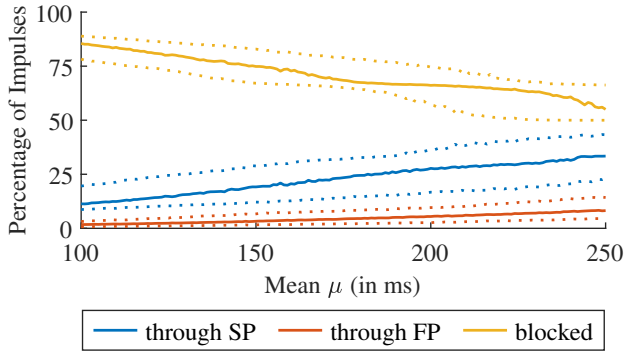

Figure 2. Percentages of conducted impulses through the SP (blue), FP (red) and blocked impulses (yellow). The graph shows the median (solid line), 25th percentile and 75th percentile over the mean μ.

Ca^{+}-blockers may be caused by differences in drug induced changes of AV conduction delay and AA properties. The fact that the majority of impulses are conducted over the SP instead of the FP (Figure 2) may explain why SP refractoriness is more important for the RR series characteristics than FP refractoriness, as indicated by the larger regression coefficients (Figure 1).

The changes in the variance of the variability and irregularity measures can only be partly explained by a linear model, R^2=34.6% and R^2=41.5% respectively. Therefore, further investigation using more advanced techniques, such as variance-based sensitivity analysis methods, is warranted.

References

[1] Hindricks G et al. 2020 ESC Guidelines for the diagnosis and management of atrial fibrillation developed in collaboration with the European Association for Cardio-Thoracic Surgery (EACTS). European Heart Journal 2020;42(5):1–126.

[2] Lei M et al. Modernized Classification of Cardiac Antiarrhythmic Drugs. Circulation 2018;138(17):1879–1896.

[3] Costea AI, Platonov PG. Rate Modulation Drugs in Atrial Fibrillation: What is the Clinical Impact? J Cardiovasc Electrophysiol 2015;26(2):142–144.

[4] George SA et al. At the Atrioventricular Crossroads: Dual Pathway Electrophysiology in the Atrioventricular Node and its underlying Heterogeneities. Arrhythmia and Electrophysiology Review 2017;6(4):179–185.

[5] Billette J, Tadros R. An integrated overview of AV node physiology. Pacing Clin Electrophysiol 2019;42(7):805–820.

[6] Henriksson M et al. A Statistical Atrioventricular Node Model Accounting for Pathway Switching during Atrial Fibrillation. IEEE Transactions on Biomedical Engineering 2016;63(9):1842–1849.

[7] Inada S et al. Simulation of ventricular rate control during atrial fibrillation using ionic channel blockers. Journal of Arrhythmia 2017;33(4):302–309.

[8] Wallman M, Sandberg F. Characterisation of human AV-nodal properties using a network model. Med Biol Eng Comput 2018;56(2):247–259.

[9] Climent AM et al. Generation of realistic atrial to atrial interval series during atrial fibrillation. Med Biol Eng Comput 2011;49(11):1261–1268.

[10] Richman JS, Randall Moorman J. Physiological time-series analysis using approximate entropy and sample entropy. Am J Physiol Heart Circ Physiol 2000;278(6):2039–2049.

[11] Denes P et al. The Effects of Cycle Length on Cardiac Refractory Periods in Man. Circulation 1974;49(1):32–41.

[12] Corino VDA et al. Rate-Control Drugs Affect Variability and Irregularity Measures of RR Intervals in Patients with Permanent Atrial Fibrillation. J Cardiovasc Electrophysiol 2015;26(2):137–141.

Address for correspondence:

Felix Plappert
Lund University, Department of Biomedical Engineering
Box 118, 221 00 Lund, Sweden
felix.plappert@bme.lth.se